

EDGE ARTICLE

View Article Online
View Journal | View IssueCite this: *Chem. Sci.*, 2021, 12, 9991

All publication charges for this article have been paid for by the Royal Society of Chemistry

Catalytic asymmetric synthesis of spirocyclobutyl oxindoles and beyond *via* [2+2] cycloaddition and sequential transformations†Xia Zhong,^{ID} Jiuqi Tan, Jianglin Qiao, Yuqiao Zhou,^{ID} Cidan Lv, Zhishan Su,^{ID} Shunxi Dong^{ID}* and Xiaoming Feng^{ID}*

Efficient asymmetric synthesis of a collection of small molecules with structural diversity is highly important to drug discovery. Herein, three distinct types of chiral cyclic compounds were accessible by enantioselective catalysis and sequential transformations. Highly regio- and enantioselective [2+2] cycloaddition of (*E*)-alkenyloxindoles with the internal C=C bond of *N*-allenamides was achieved with *N,N'*-dioxide/Ni(OTf)₂ as the catalyst. Various optically active spirocyclobutyl oxindole derivatives were obtained under mild conditions. Moreover, formal [4+2] cycloaddition products occurring at the terminal C=C bond of *N*-allenamides, dihydropyran-fused indoles, were afforded by a stereospecific sequential transformation with the assistance of a catalytic amount of Cu(OTf)₂. In contrast, performing the conversion under air led to the formation of γ -lactones *via* the water-involved deprotection and rearrangement process. Experimental studies and DFT calculations were performed to probe the reaction mechanism.

Received 17th May 2021
Accepted 22nd June 2021

DOI: 10.1039/d1sc02681j

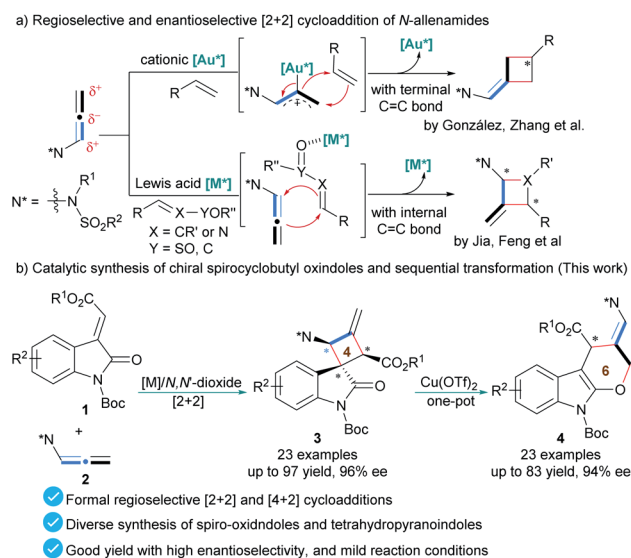
rsc.li/chemical-science

Introduction

Diversity-oriented synthesis (DOS)¹ aims to create a library of small molecules with structural complexity and diversity in an efficient manner. Over the past two decades, great endeavors have been devoted to developing new methods and strategies towards this goal.² Sequential reactions of chiral molecules generated *in situ* from asymmetric catalysis greatly enriched the chemical space,³ but discovering such synthons and convenient conditions without erosion of stereoselectivity remains challenging. *N*-Allenamides have attracted considerable interest as a versatile reagent in organic synthesis.⁴ Structurally, the amide moiety in *N*-allenamides is critical to strike the right balance between their reactivity and stability. This special structure endows *N*-allenamides with unique reactivity in diverse transformations,^{4a,b,5} such as addition reactions, cycloadditions and so on. Interestingly, both internal and terminal C=C bonds of *N*-allenamides have been disclosed in cycloaddition reactions^{4b-e,6} including asymmetric versions^{4d} (Scheme 1a). The regioselectivity of allenes depends on the choice of the catalyst,⁷ substrate⁸ and the

substituent on the amide group.⁹ These impressive features make *N*-allenamides a promising substrate in diversity-oriented synthesis.

Cyclobutane is present in many biologically active compounds,¹⁰ and is also an appealing building block in synthetic organic chemistry.¹¹ Among a number of protocols for the synthesis of cyclobutanes,¹² the [2+2] cycloaddition

Scheme 1 Asymmetric [2+2] cycloadditions of *N*-allenamides.

Key Laboratory of Green Chemistry & Technology, Ministry of Education, College of Chemistry, Sichuan University, Chengdu 610064, China. E-mail: dongs@scu.edu.cn; xmfeng@scu.edu.cn; Web: http://www.scu.edu.cn/chem_asl/

† Electronic supplementary information (ESI) available: ¹H, ¹³C{¹H} and ¹⁹F{¹H} NMR spectra, HPLC chromatograms, and CD spectra (PDF). X-ray crystallographic data for **3aa**, **rac-4ka** and **rac-5aa**. CCDC 2042864, 2052253 and 2079315. For ESI and crystallographic data in CIF or other electronic format see DOI: 10.1039/d1sc02681j



represents one of most powerful strategies due to its high efficiency and stereoselectivity.^{12d-f} In this context, the [2+2] cycloadditions of olefins with either terminal or internal C=C bonds of *N*-allenamides have been accomplished by using a chiral cationic Au(I) catalyst¹³ or Lewis acid catalyst¹⁴ (Scheme 1a). Considering the frequent occurrence of the spirocyclobutyl oxindole skeleton in bioactive molecules,^{12h-j,15} it is highly desirable to develop reliable access to spirocyclobutyl oxindole derivatives.¹⁶ In continuation with our interest in chiral *N,N'*-dioxide/metal Lewis acid catalysis¹⁷ and inspired by elegant studies^{5,13,14} on the *N*-allenamide chemistry, herein, we demonstrated that catalysts could promote the direct asymmetric [2+2] cycloaddition of (*E*)-alkenyloxindoles with *N*-allenamides for straightforward access to optically active spirocyclobutyl oxindole derivatives (Scheme 1b). Moreover, further diversified transformation¹⁸ of the internal C=C bond-involved product catalyzed by a copper salt enabled the one-pot synthesis of tetradropyranoxindole derivatives, which seem to be the formal [4+2] cycloaddition adducts of the terminal C=C bond of *N*-allenamides. Further transformation in the presence of acid and water gave 4'-methylenedihydrofuranone-substituted oxindole derivatives.

Table 1 Optimization of the reaction conditions^a

Ar = 2,6-*i*-Pr₂C₆H₃

L₃-PiPr₂: n = 2, m = 1
 L₂-PiPr₂: n = 2, m = 0
 L₄-PiPr₂: n = 2, m = 2
 L₄-PrPr₂: n = 1, m = 2

L₄-RaPr₂: m = 2
 L₅-RaPr₂: m = 3

L1

L2

Entry	Ligand	Yield of (3aa + 4aa) ^b (%)	3aa : 4aa ^c	3aa	4aa
1	w/o	13	1 : 99	—	0
2	L ₃ -PiPr ₂	58	89 : 11	91	51
3 ^d	L ₃ -PiPr ₂	39	1 : 99	—	60
4	L ₂ -PiPr ₂	59	60 : 40	58	83
5	L ₄ -PiPr ₂	55	97 : 3	95	—
6	L ₄ -PrPr ₂	55	98 : 2	79	—
7	L ₄ -RaPr ₂	75	97 : 3	90	—
8	L ₅ -RaPr ₂	74	98 : 2	95	—
9 ^e	L ₅ -RaPr ₂	94	98 : 2	95	—
10	L1	29	1 : 99	—	0
11	L2	33	1 : 99	—	—11

^a Unless otherwise noted, all reactions were carried out with **1a** (0.05 mmol), **2a** (1.0 equiv.), and ligand/Ni(OTf)₂ (1 : 1, 10 mol%) in CH₂Cl₂ (0.1 M) at 30 °C for 16 h under N₂. ^b Isolated yield of **3aa** and **4aa**. ^c Determined by HPLC on a chiral stationary phase. ^d Ligand/Ni(OTf)₂ (1 : 1.5). ^e **2a** (1.2 equiv.) in CH₂Cl₂ (0.2 M) at 35 °C. Ts = *p*-tosyl.

Results and discussion

Initially, (*E*)-alkenyloxindole **1a** and *N*-allenamide **2a** were selected as the model substrates. The key reaction condition optimization is listed in Table 1 (for more details, see the ESI†). In the preliminary screening, only tetradropyranoxindole derivative **4aa**, the formal [4+2] cycloaddition product¹⁹ reacting at the terminal C=C bond of *N*-allenamide, was obtained in the presence of Ni(OTf)₂ (entry 1, 13% yield). Interestingly, when the reaction was performed by the use of the chiral L₃-PiPr₂/Ni^{II} complex, the [2+2] cycloaddition reaction took place smoothly, affording the corresponding internal C=C bond involved spirocyclobutyl oxindole **3aa** as the major product with 91% ee (**3a** : **4a** = 89 : 11, in total 58% yield; entry 2). It is worth mentioning that when excessive amounts of the metal salt existed in the catalytic system with the chiral ligand, it led to the exclusive isolation of the product **4aa** in 39% yield and 60% ee (entry 3). The examination of ligands suggested that the length of the carbon tether has a significant effect on the reaction, and the longer linker of *N,N'*-dioxide resulted in better chemoselectivity and enantioselectivity (entries 2, 4 and 5, the ratio of **3aa** to **4aa**, from 60 : 40 to 97 : 3). Variation of the chiral backbone exhibited that (*S*)-2-pipecolic acid derived L₄-PiPr₂ gave better enantioselectivity, while L-ramipril derived L₄-RaPr₂ resulted in a higher yield and comparable ee value (entries 5–7). The level of enantioselectivity increased to 95% ee when L₅-RaPr₂ with a five-carbon tether was used as the ligand (entry 8). We also identified other parameters for this asymmetric [2+2] cycloaddition reaction (see ESI, Tables S1–S4† for details), and 94% yield and 95% ee were obtained when 1.2 equivalents of **2a** were used at higher temperature and concentration (entry 9). It

Table 2 Optimization of Lewis acids for the sequential reaction^a

Entry	Metal salt	Yield ^b (%)	3aa : 4aa ^c	ee of 4aa ^c (%)
1	Ni(OTf) ₂	76	82 : 18	92
2	Zn(OTf) ₂	54	6 : 94	91
3	Mg(OTf) ₂	52	34 : 66	91
4	Cu(OTf) ₂	49	1 : 99	93
5 ^d	Cu(OTf) ₂	70	1 : 99	93
6 ^e	Cu(OTf) ₂	70	1 : 99	93

^a Unless otherwise noted, all reactions were initially carried out with **1a** (0.05 mmol), **2a** (1.2 equiv.), L₅-RaPr₂ (10 mol%) and Ni(OTf)₂ (10 mol%) in CH₂Cl₂ (0.2 M) at 35 °C for 16 h. Then, the metal salt (5 mol%) in CH₂Cl₂ (0.1 M) was added and stirred at 30 °C for 16 h under air.

^b Isolated yield of **4aa** based on **1a**. ^c Determined by HPLC on a chiral stationary phase. ^d 4 Å MS (10 mg) in CHCl₃ (0.05 M) was used for the second transformation for 3 h. ^e Isolated **3aa** was treated with Cu(OTf)₂ (5 mol%) and 4 Å MS (10 mg) in CHCl₃ (0.05 M) at 30 °C for 4 h under N₂.

should be noted that the use of other ligands, such as BINOL **L1** or oxazoline **L2**, only led to the formation of [4+2] cycloaddition product **4aa** in moderate yield with a low ee value (entries 10 and 11). Noteworthy, the diastereoselectivity of [2+2] cycloaddition was very high as only one diastereomer was detected in all cases.

It was observed that the presence of the metal salt (Table 1, entry 1 and 3) led to the formation of **4aa**. The control experiment showed that the isolated spirocyclobutyl oxindole **3aa** could be transformed into **4aa** in 37% yield accompanied by a tiny amount of the by-product by treatment with 5 mol% of Ni(OTf)₂ after 16 h under an air atmosphere (See ESI, Table S5 and Fig. S4† for more details). In contrast, [4+2] product **4aa** did not transform into the spirocyclobutyl oxindole **3aa** at all under the same conditions. It was indicated that the [2+2] cycloaddition occurred initially, followed by an achiral Lewis acid-accelerated rearrangement to yield tetradropyranindole **4aa**. Further investigation of other Lewis acids for a one-pot sequential reaction (Table 2), such as, Ni(OTf)₂, Mg(OTf)₂, Zn(OTf)₂ or Cu(OTf)₂, manifested that Cu(OTf)₂ performed better (Table 2, entries 1–4). When 4 Å MS was added as a water scavenger, the total yield of **4aa** increased to 70% in CHCl₃ (entry 5), and the formation of the byproduct was obviously reduced. During these procedures, the enantioselectivity of the product **4aa** was high and 93% ee was obtained after Cu(OTf)₂ promoted sequential transformation. The result of one-pot sequential reactions was nearly the same as the two-step transformation (entry 6 vs. entry 5).

With the optimized reaction conditions in hand, the substrate scopes to synthesize chiral spirocyclobutyl oxindoles *via* chiral nickel(II) complex catalyzed [2+2] cycloaddition, and to synthesize tetradropyranindoles *via* one-pot sequential transformation were investigated (Table 3). The effects of the ester groups of (*E*)-alkenyloxindole were first evaluated, and both yields and ee values were elevated gradually with the increase of steric hindrance of the ester group (**3aa**–**3ea**). The substrates with different substituents on the indole ring at the C5, C6, and C7 positions took part in the reaction smoothly, providing the desired spirocyclobutyl oxindoles **3fa**–**3pa** in 72–94% yield with 87–96% ee. Moreover, the C5,C6-difluoro substituted alkenyloxindole was also applicable, affording **3qa** in 76% yield and 92% ee. Subsequently, we turned our attention to the scope of *N*-allenamides **2**. Various substituted *N*-allenamides were suitable in the current system, giving the corresponding products in good yields and excellent enantioselectivities (**3ab**–**3ag**, 69–97% yield, and 93–96% ee). The absolute configuration of product **3aa** was determined to be (1*R*,2*R*,4*S*) by X-ray crystallography analysis,²⁰ and the others were assigned by comparing their CD spectra with that of **3aa** (see the ESI† for details). In comparison, the trend of enantioselectivity of the products **4** was similar to that of the corresponding spirocyclobutyl oxindoles. As depicted in Table 3, (*E*)-alkenyloxindoles and *N*-allenamides transformed into the tetradropyranindoles in 33–83% yields and 70–93% ee after one-pot sequential transformation. The absolute configuration of **4ka** was assigned as (*R*,*E*) on the basis of the absolute configuration of **3ka** and the relative configuration of racemic **4ka**.²⁰

Table 3 Substrate scopes^a

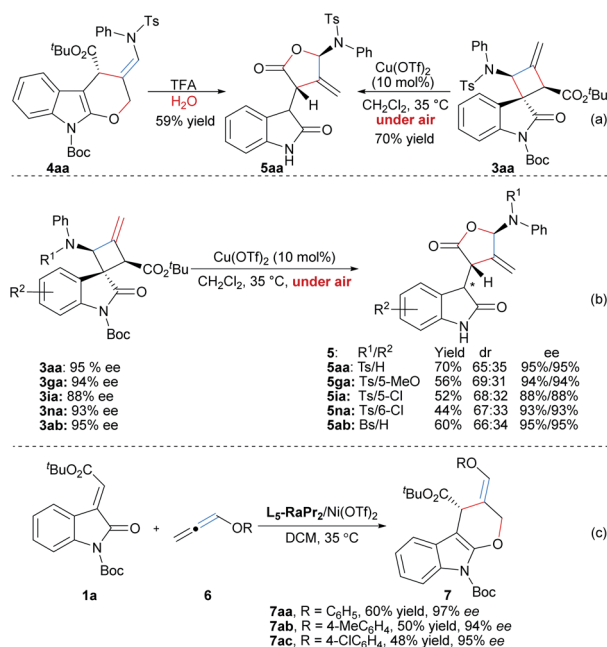
Product	Yield (%)	ee (%)
3aa , R = ^t Bu	93	95
3ba , R = Me	85	70
3ca , R = Et	86	78
3da , R = ⁱ Pr	93	93
3ea , R = Bn	93	81
3fa , R = 5-Me	91	93
3ga , R = 5-MeO	94	94
3ha , R = 5-F	77	92
3ia , R = 5-Cl	72	88
3ja , R = 5-Br	81	88
3ka , R = 5-I	83	90
3ab , R = Ph	94	95
3ac , R = 4-MeOC ₆ H ₄	88	95
3ad , R = 4- ^t BuC ₆ H ₄	85	95
3ae , R = 1-naphthyl	96	94
3af , R = Me	69	96
3ag , R = 4-MeC ₆ H ₄	97	93
4aa , R = ^t Bu	70	93
4ba , R = Me	73	70
4ca , R = Et	83	78
4da , R = ⁱ Pr	71	93
4ea , R = Bn	64	83
4fa ^d , R = 5-Me	72	91
4ga , R = 5-MeO	79	92
4ha , R = 5-F	67	92
4ia , R = 5-Cl	55	89
4ja , R = 5-Br	61	88
4ka , R = 5-I	57	90
4la ^d , R = 6-MeO	33	91
4ma , R = 6-F	62	93
4na , R = 6-Cl	54	90
4oa , R = 6-Br	57	88
4pa , R = 7-Cl	61	94
4qa , R = 5,6-F ₂	57	90
4ab ^d , R = Ph	71	92
4ac ^d , R = 4-MeOC ₆ H ₄	63	93
4ad ^d , R = 4- ^t BuC ₆ H ₄	75	91
4ae ^d , R = 1-naphthyl	83	90
4af ^d , R = Me	40	93
4ag , R = 4-MeC ₆ H ₄	71	93

cond. 1: *L*₂-**RaPr**₂/Ni(OTf)₂, CH₂Cl₂, 35 °C, 16 h
cond. 2: Cu(OTf)₂ (5 mol%), 4 Å MS, CHCl₃, 30 °C

^a Unless otherwise noted, the [2+2] cycloaddition conditions were the same as in Table 1, entry 8; and the synthesis of product **4** followed the same procedure as in Table 2, entry 5. Isolated yields of **3** and **4** are based on **1**. The ee value was determined by HPLC on a chiral stationary phase. ^b Cu(OTf)₂ (10 mol%). ^c Cu(OTf)₂ (7.5 mol%). ^d **4fa** : **3fa** = 19 : 1. ^e **4la** : **3la** = 9 : 1. ^f Cu(OTf)₂ (12.5 mol%).

The structure of byproduct **5aa** accompanied by the formation of **4aa** in the sequential reaction was determined to be a γ -lactone derivative by X-ray crystal diffraction analysis.²⁰ We proposed that γ -lactone **5aa** was probably generated *via* water-involved hydrolysis with concomitant deprotection of the *N*-Boc group, following rearrangement (mechanism explanation is shown in Fig. 2b, cycle B). Interestingly, treatment of spirocyclobutyl oxindole **3aa** with Cu(OTf)₂ under air afforded γ -lactone **5aa** with sharply improved yield (Scheme 2a; 70%, 65 : 35 dr, 95% ee for each diastereomer). Moreover, exposure of product **4aa** to trifluoroacetic acid (TFA) also led to the formation of **5aa** in 59% yield, 65 : 35 dr and 95% ee for each diastereomer (Scheme 2a). Subsequently, the conversion of spirocyclobutyl oxindoles **3** to γ -lactone substituted oxindoles **5** was examined (Scheme 2b).²¹ Under the influence of Cu(OTf)₂, [2+2] products **3** with different substituents transformed into the corresponding products **5** in moderate yields and diastereoselectivities (44–70% yield, 65 : 35–69 : 31 dr) without any loss of enantioselectivity. The poor diastereoselectivity is due to





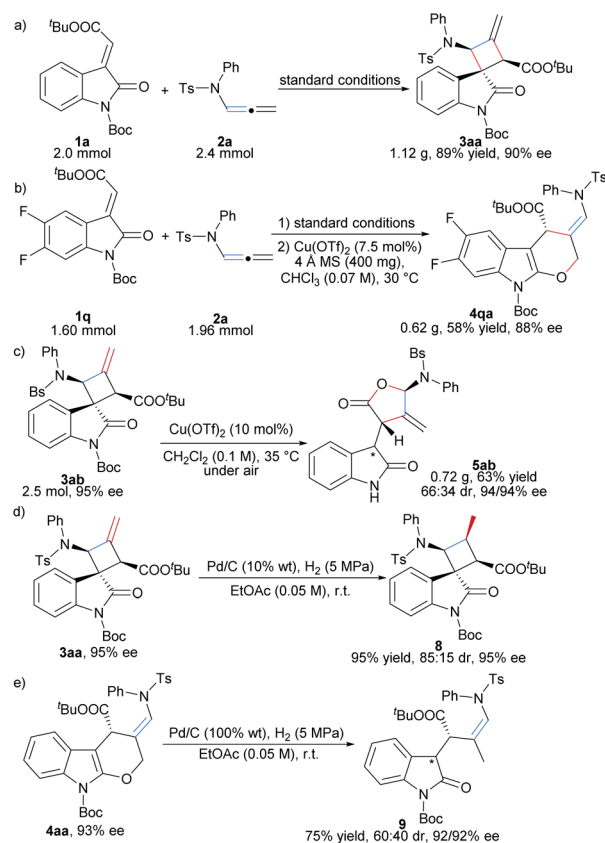
Scheme 2 The preparation of 4'-methylenedihydrofuranone-substituted oxindoles **5** and dihydropyran-fused indole products **7**.

the epimerization balance at the C3-position of oxindoles, and stereochemistry at the γ -lactone structure was maintained.

Alkoxyallenes **6** were turned out to be suitable reaction partners. In these cases, [4+2] products **7** were obtained directly without the detection of the [2+2] cycloaddition products in the reaction system (see ESI, Table S10† for details). As shown in Scheme 2c, representative examples of alkoxyallenes **6** were tested, and all the reactions proceeded well, providing the corresponding dihydropyran-fused indole products in moderate yields and excellent enantioselectivities (**7aa–7ac**, 48–60% yield, and 94–97% ee).

To show the potential synthetic utility of the current method, scale-up synthesis of **3aa**, **4qa** and **5ab** was carried out. Under the optimized reaction conditions, **1a** (2.0 mmol) reacted with **2a** (2.4 mmol) smoothly, providing the spirocyclobutyl oxindole **3aa** in 89% yield (1.12 g) with 90% ee (Scheme 3a). It should be noted that for the synthesis of dihydropyran-fused indole product **4qa**, increasing the amount of Cu(OTf)₂ (7.5 mol%) and 4 Å MS, and the reaction concentration (0.07 M) was necessary to get high yield (58% yield for two steps) in 88% ee by employing 1.60 mmol **1q** (Scheme 3b). γ -Lactone **5ab** was obtained in 63% yield (0.72 g), 66 : 34 dr and 94% ee for each diastereomer (Scheme 3c). Furthermore, hydrogenation of **3aa** in the presence of Pd/C and H₂ gave rise to densely substituted spirocyclobutyl oxindole **8** in 95% yield, 85 : 15 dr and 95% ee (Scheme 3d). Hydrogenation of **4aa** resulted in C–O bond cleavage of the pyran ring, delivering the product **9** in 75% yield, 60 : 40 dr and 92/92% ee (Scheme 3e).

To probe the mechanism for the transformation, the Cu(OTf)₂-catalyzed isomerizations from **3aa** to **E-4aa** or **Z-4aa** were studied at the M06-D3/6-31G(d,p) (SMD, dichloromethane) theoretical level and the energy profiles are shown in Fig. 1 (see



Scheme 3 Scale-up reactions and further transformations of the products.

ESI,† computational details part for more details). **3aa** coordinated to Cu(OTf)₂ in a bidentate fashion, forming an intermediate **IM1**. This process was exothermic by 25.5 kcal mol^{−1}. Then, it underwent a ring-opening process *via* transition state **TS1**, generating intermediate **I**. Suffering from the steric repulsion from the OTf[−] anion in the catalyst, the relative Gibbs free energy of intermediate **II** with *s-cis*-unsaturated imine **s-cis-II** was slightly higher than that with the *s-trans*-one by 0.8 kcal mol^{−1}. In the following step, the C–O bond in **E-IM2** was constructed *via* transition state **E-TS2**, with ΔG^\ddagger of 12.3 kcal mol^{−1}. In contrast, the activation barrier associated with the formation of **Z-IM2** *via* **Z-TS2** was 14.3 kcal mol^{−1}. In addition, **Z-IM2** was less stable than **E-IM2** by 5.0 kcal mol^{−1}. These results indicated that **E-4aa** was predominantly formed in the presence of Cu(OTf)₂. Although heating **3aa** in DCE at 80 °C for 24 h led to the generation of **E-4aa**, the DFT studies indicated that the presence of Cu(OTf)₂ could accelerate this conversion with low activation barriers (12.8 and 12.3 kcal mol^{−1}), thus making the reaction possible at 30 °C (see ESI, Fig. S5† for more details).

Based on the above analysis and the X-ray crystal structures of product **3aa** and the L₃-PiPr₂/Ni^{II} complex,²² a possible working mode was proposed to elucidate the stereoselectivity of the [2+2] reaction. As shown in Fig. 2a, chiral *N,N'*-dioxide and alkenyloxindole **1a** coordinated to Ni^{II} in tetradentate and bidentate fashions respectively to form a slightly distorted



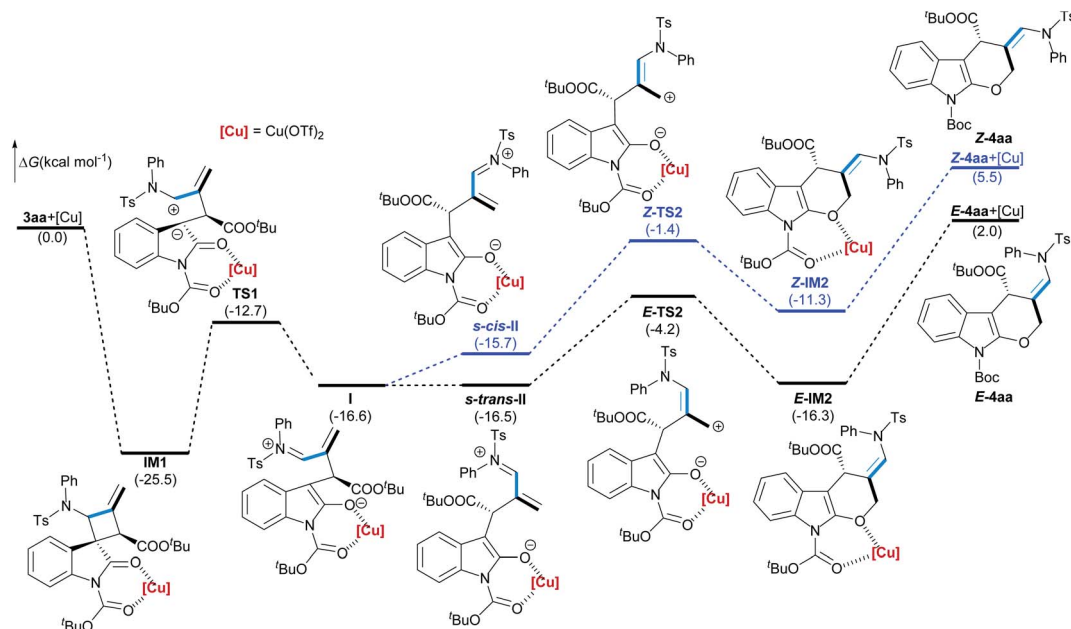


Fig. 1 Energy profiles for the isomerization from **3aa** to **E-4aa** or **Z-4aa** catalyzed by $\text{Cu}(\text{OTf})_2$.

hexahedral complex. The Si-face of the substrate **1a** was shielded by the substituted aniline group on the ligand. Consequently, *N*-allenamide **2a** approached from its β -Re-face to form the zwitterionic intermediate, followed by cyclization from the Re-face of the imine moiety to afford [2+2] cycloaddition adduct (1*R*,2*R*,4*S*)-**3aa**.

When Lewis acid $\text{Cu}(\text{OTf})_2$ comes into contact with [2+2] adduct **3aa**, it will bond the *N*-Boc oxindole in a bidentate manner, leading to ring opening of the strained cyclobutyl structure to deliver the zwitterionic intermediate **I** (Fig. 1). Then the isomerization of intermediate **I** provided unsaturated imine

s-trans-II, which was trapped by the intramolecular Lewis acid-bonded enol anion to generate the dihydropyran-fused indole product **E-4aa**. This reaction pathway was rationalized by DFT studies as well (see ESI, Fig. S11–S13† for more details). During the process, the stereocenter at the ester substituent is unaffected, and thus the enantioselectivity of **4aa** is maintained. On the other hand, when **3aa** was isolated and the second step was performed under an air atmosphere, after the formation of intermediate **I**, deprotection of the Boc group and hydrolysis of the ester unit successively take place under the influence of Lewis acid $\text{Cu}(\text{OTf})_2$,^{3c,23} affording the acid intermediate **III**. Subsequently, diastereoselective intramolecular Mannich-type cyclization and proton transfer occurs, yielding the lactone product **5aa** with high enantioselectivity (Fig. 2b, cycle A). Moreover, treatment of product **4aa** with TFA gave rise to intermediate **V**, which underwent ring-opening and proton transfer to produce **5aa** (Fig. 2b cycle B, see ESI, Fig. S6† for more details).

Conclusions

In summary, we have successfully developed a highly enantioselective [2+2] cycloaddition reaction between the internal C=C bond of *N*-allenamides and (*E*)-alkenyloxindole catalyzed by a chiral $\text{L}_5\text{-RaPr}_2/\text{Ni}(\text{OTf})_2$ catalyst. The appropriate steric and electronic properties of the catalyst enable the controllable formation of chiral spirocyclobutyl oxindole derivatives in good yields with high stereoselectivities, suppressing the rearrangement into thermodynamically stable formal [4+2] adducts. Nevertheless, diversity-oriented synthesis *via* sequential transformations was available, such as dihydropyran-fused indoles and lactones from chiral spirocyclobutyl oxindoles, which could be performed in a one-pot manner by the use of additional

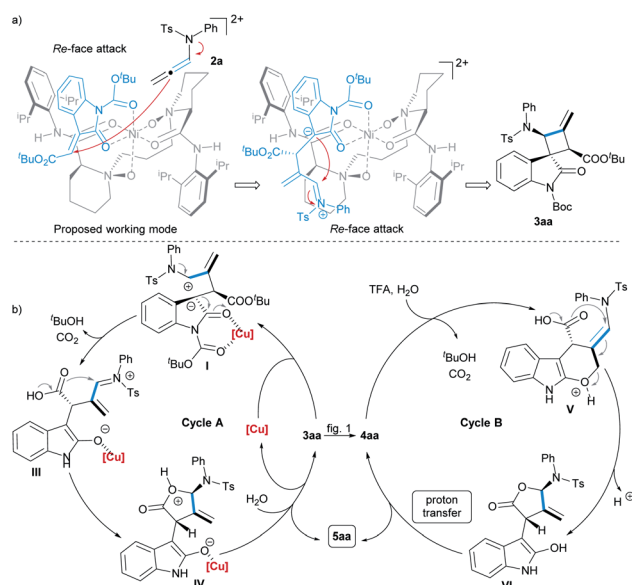


Fig. 2 Proposed transition state model and mechanism.



copper salt in the absence or presence of water. On the basis of control experiments and DFT studies, plausible transition state model and catalytic cycles were proposed to explain the origin of chem- and stereoselective control and transformation processes. The synthesis of three different kinds of enantioenriched cyclic compounds from the same starting materials and chiral catalysts makes the current methodology attractive.

Data availability

Further details of experimental procedure, ^1H , $^{13}\text{C}\{^1\text{H}\}$ and $^{19}\text{F}\{^1\text{H}\}$ NMR, HPLC spectra, SFC spectra, CD spectra, computational methods and X-ray crystallographic data for **3aa**, **rac-4ka** and **rac-5aa** are available in the ESI.

Author contributions

X. Z. and J. L. Q. performed the experiments. J. Q. T. repeated data. C. D. L. and Z. S. S. analyzed the computational data. S. X. D. participated in structure characterization and discussion. Y. Q. Z. analyzed the X-ray diffraction crystal data. X. M. F. and X. H. L. supervised the project. X. M. F., X. H. L., S. X. D. and X. Z. co-wrote the manuscript.

Conflicts of interest

There are no conflicts to declare.

Acknowledgements

We acknowledge the National Natural Science Foundation of China (No. 21772127 and 21921002) for financial support.

Notes and references

- (a) M. D. Bruke and S. L. Schreiber, *Angew. Chem., Int. Ed.*, 2004, **43**, 46; (b) C. J. O' Connor, H. S. Beckmann and D. R. Spring, *Chem. Soc. Rev.*, 2012, **41**, 4444; (c) K. T. Mortensen, T. J. Osberger, T. A. King, H. F. Sore and D. R. Spring, *Chem. Rev.*, 2019, **119**, 10288.
- (a) D. Tan, *Nat. Chem. Biol.*, 2005, **1**, 74; (b) W. R. Galloway, A. Isidro-Llobet and D. R. Spring, *Nat. Commun.*, 2010, **1**, 80.
- For reviews, see: (a) S. L. Schreiber, *Science*, 2000, **287**, 1964; (b) G. Moura-Letts, C. M. DiBlasi, R. A. Bauer and D. S. Tan, *Proc. Natl. Acad. Sci. U. S. A.*, 2011, **108**, 6745. For selected examples, see: (c) H. F. Zheng, Y. Wang, C. R. Xu, Q. Xiong, L. L. Lin and X. M. Feng, *Angew. Chem., Int. Ed.*, 2019, **58**, 5327; (d) D. Zhang, Z. S. Su, Q. W. He, Z. K. Wu, Y. Q. Zhou, C. J. Pan, X. H. Liu and X. M. Feng, *J. Am. Chem. Soc.*, 2020, **142**, 15975; (e) X. Lin, Y. Liu and C. Li, *Chem.-Eur. J.*, 2020, **26**, 14173.
- For reviews, see: (a) L.-L. Wei, H. Xiong and R. P. Hsung, *Acc. Chem. Res.*, 2003, **36**, 773; (b) T. Lu, Z. Lu, Z.-X. Ma, Y. Zhang and R. P. Hsung, *Chem. Rev.*, 2013, **113**, 4862; (c) M. R. Frutos and A. Prieto, *Tetrahedron*, 2016, **72**, 355; (d) E. Manoni and M. Bandini, *Eur. J. Org. Chem.*, 2016, 3135; (e) C. Praveen, *Catal. Rev.*, 2019, **61**, 406.
- (a) W. B. Dickinson and P. C. Lang, *Tetrahedron Lett.*, 1967, **8**, 3035; (b) S. Ma, in *Modern Allene Chemistry*, ed. A. S. K. Hashmi, Wiley-VCH, Weinheim, 2004, vol. 1–2, p. 595.
- For selected examples, see: (a) W. Zhou, X.-X. Li, G.-H. Li, Y. Wu and Z. Chen, *Chem. Commun.*, 2013, **49**, 3552; (b) G.-H. Li, W. Zhou, X.-X. Li, Q.-W. Bi, Z. Wang, Z.-G. Zhao, W.-X. Hu and Z. Chen, *Chem. Commun.*, 2013, **49**, 4770; (c) S. Montserrat, H. Faustino, A. Lledós, J. L. Mascareñas, F. López and G. Ujaque, *Chem.-Eur. J.*, 2013, **19**, 15248; (d) V. Pirovano, L. Decataldo, E. Rossi and R. Vicente, *Chem. Commun.*, 2013, **49**, 3594; (e) H. Faustino, I. Alonso, J. L. Mascareñas and F. López, *Angew. Chem., Int. Ed.*, 2013, **52**, 6526; (f) P. Bernal-Albert, H. Faustino, A. Gimeno, G. Asensio, J. L. Mascareñas and F. López, *Org. Lett.*, 2014, **16**, 6196; (g) H. Faustino, I. Varela, J. L. Mascareñas and F. López, *Chem. Sci.*, 2015, **6**, 2903; (h) E. López, J. González and L. A. López, *Adv. Synth. Catal.*, 2016, **358**, 1428; (i) S. Peng, D. Ji and J. Sun, *Chem. Commun.*, 2017, **53**, 12770; (j) N. De, C. E. Song, D. H. Ryu and E. J. Yoo, *Chem. Commun.*, 2018, **54**, 6911; (k) D. C. Marcote, I. Varela, J. Fernández-Casado, J. L. Mascareñas and F. López, *J. Am. Chem. Soc.*, 2018, **140**, 16821; (l) C. Wang, G. Xu, Y. Shao, S. Tang and J. Sun, *Org. Lett.*, 2020, **22**, 5990.
- J. M. Wiest, M. L. Conner and M. K. Brown, *J. Am. Chem. Soc.*, 2018, **140**, 15943.
- S. Peng, S. Cao and J. Sun, *Org. Lett.*, 2017, **19**, 524.
- M. Yang, L. Kang and S. He, *Heterocycles*, 2019, **98**, 1725.
- (a) *The Chemistry of Cyclobutanes*, ed. Z. Rappoport and J. F. Liebman, Wiley, Chichester, 2005; (b) A. Fernández-Tejada, F. Corzana, J. H. Busto, G. Jiménez-Osés, J. M. Peregrina and A. Avenoza, *Chem.-Eur. J.*, 2008, **14**, 7042; (c) K.-G. Wen, Y.-Y. Peng and X.-P. Zeng, *Org. Chem. Front.*, 2020, **7**, 2576; (d) M. R. Bauer, P. Di Fruscia, S. C. C. Lucas, I. N. Michaelides, J. E. Nelson, R. I. Storer and B. C. Whitehurst, *RSC Med. Chem.*, 2021, **12**, 448.
- For selected reviews, see: (a) J. C. Namyslo and D. E. Kaufmann, *Chem. Rev.*, 2003, **103**, 1485; (b) E. Leemans, M. D'hooghe and N. De Kimpe, *Chem. Rev.*, 2011, **111**, 3268; (c) T. Seiser, T. Saget, D. N. Tran and N. Cramer, *Angew. Chem., Int. Ed.*, 2011, **50**, 7740. For selected examples, see: (d) B.-S. Li, W.-X. Liu, Q.-W. Zhang, S.-H. Wang, F.-M. Zhang, S.-Y. Zhang, Y.-Q. Tu and X.-P. Cao, *Chem.-Eur. J.*, 2013, **19**, 5246; (e) B.-M. Yang, P.-J. Cai, Y.-Q. Tu, Z.-X. Yu, Z.-M. Chen, S.-H. Wang, S.-H. Wang and F.-M. Zhang, *J. Am. Chem. Soc.*, 2015, **137**, 8344; (f) W. Mazumdar, N. Jana, B. T. Thurman, D. J. Wink and T. G. Driver, *J. Am. Chem. Soc.*, 2017, **139**, 5031; (g) J. Guo, X. Xu, Q. Xing, Z. Gao, J. Gou and B. Yu, *Org. Lett.*, 2018, **20**, 7410; (h) M.-H. Xu, K.-L. Dai, Y.-Q. Tu, X.-M. Zhang, F.-M. Zhang and S.-H. Wang, *Chem. Commun.*, 2018, **54**, 7685; (i) F.-S. He, Y. Wu, X. Li, H. Xia and J. Wu, *Org. Chem. Front.*, 2019, **6**, 1873; (j) Y. Kim and D. Y. Kim, *Bull. Korean Chem. Soc.*, 2021, **42**, 510; (k) H. Zheng, R. Wang, K. Wang, D. Wherritt, H. Arman and M. P. Doyle, *Chem. Sci.*, 2021, **12**, 4819.
- (a) E. Lee-Ruff and G. Mladenova, *Chem. Rev.*, 2003, **103**, 1449; (b) V. M. Dembitsky, *Phytomedicine*, 2014, **21**, 1559;



- (c) J.-P. Deprés, P. Delair, J.-F. Poisson, A. Kanazawa and A. E. Greene, *Acc. Chem. Res.*, 2016, **49**, 252; (d) G. Otárola, J. J. Vaquero, E. Merino and M. A. Fernández-Rodríguez, *Catalysts*, 2020, **10**, 1178; (e) F. Secci, A. Frongia and P. P. Piras, *Molecules*, 2013, **18**, 15541; (f) Y. Xu, M. L. Conner and M. K. Brown, *Angew. Chem., Int. Ed.*, 2015, **54**, 11918; (g) S. Poplata, A. Tröster, Y.-Q. Zou and T. Bach, *Chem. Rev.*, 2016, **116**, 9748; (h) A. Ding, M. Meazza, H. Guo, J. W. Yang and R. Rios, *Chem. Soc. Rev.*, 2018, **47**, 5946; (i) G.-J. Mei and F. Shi, *Chem. Commun.*, 2018, **54**, 6607; (j) A. J. Boddy and J. A. Bull, *Org. Chem. Front.*, 2021, **8**, 1026.
- 13 For selected examples of [2+2] cycloadditions accomplished using a chiral cationic Au(I) catalyst, see: (a) S. Suárez-Pantiga, C. Hernández-Díaz, E. Rubio and J. M. González, *Angew. Chem., Int. Ed.*, 2012, **51**, 11552; (b) M. Jia, M. Monari, Q.-Q. Yang and M. Bandini, *Chem. Commun.*, 2015, **51**, 2320; (c) Y. Wang, P. Zhang, Y. Liu, F. Xia and J. Zhang, *Chem. Sci.*, 2015, **6**, 5564; (d) H. Hu, Y. Wang, D. Qian, Z.-M. Zhang, L. Liu and J. Zhang, *Org. Chem. Front.*, 2016, **3**, 759.
- 14 (a) R.-R. Liu, J.-P. Hu, J.-J. Hong, C.-J. Lu, J.-R. Gao and Y.-X. Jia, *Chem. Sci.*, 2017, **8**, 2811; (b) X. Zhong, Q. Tang, P. F. Zhou, Z. W. Zhong, S. X. Dong, X. H. Liu and X. M. Feng, *Chem. Commun.*, 2018, **54**, 10511; (c) W.-F. Zheng, G.-J. Sun, L. Chen and Q. Kang, *Adv. Synth. Catal.*, 2018, **360**, 1790; (d) Y. Wang, P. Zhang, D. Qian and J. Zhang, *Angew. Chem., Int. Ed.*, 2015, **54**, 14849.
- 15 For selected examples, see: (a) V. M. Dembitsky, *J. Nat. Med.*, 2008, **62**, 1; (b) A. Tahri, S. M. H. Vendeville, T. H. M. Jonckers, P. J.-M. B. Raboisson, L. Hu, S. D. Demin and L. P. Cooy-Mans, *PCT Int. Appl.*, WO2014060411A, 2014; (c) A. Fensome, R. Bender, J. Cohen, M. A. Collins, V. A. Mackner, L. L. Miller, J. W. Ullrich, R. Winneker, J. Wrobel, P. Zhang, Z. Zhang and Y. Zhu, *Bioorg. Med. Chem. Lett.*, 2002, **12**, 3487; (d) M. Yoshikawa, H. Kamisaki, J. Kunitomo, H. Oki, H. Kokubo, A. Suzuki, T. Ikemoto, K. Nakashima, N. Kamiguchi, A. Harada, H. Kimura and T. Taniguchi, *Bioorg. Med. Chem.*, 2015, **23**, 7138; (e) R. K. Ujjinamatada, S. Samajdar, C. Abbineni, S. Mukeherjee, T. Linnanen and G. Wohlfahrt, *PCT Int. Appl.*, WO2016203112A1, 2016.
- 16 For selected asymmetric synthesis examples of spirocyclobutyl oxindoles, see: (a) X. Y. Hao, X. H. Liu, W. Li, F. Tan, Y. Y. Chu, X. H. Zhao, L. L. Lin and X. M. Feng, *Org. Lett.*, 2014, **16**, 134; (b) H.-M. Zhang, Z.-H. Gao and S. Ye, *Org. Lett.*, 2014, **16**, 3079; (c) L.-W. Qi, Y. Yang, Y.-Y. Gui, Y. Zhang, F. Chen, F. Tian, L. Peng and L.-X. Wang, *Org. Lett.*, 2014, **16**, 6436; (d) K. S. Halskov, F. Kniep, V. H. Lauridsen, E. H. Iversen, B. S. Donslund and K. A. Jørgensen, *J. Am. Chem. Soc.*, 2015, **137**, 1685; (e) S. S. Guo, P. Dong, Y. S. Chen, X. M. Feng and X. H. Liu, *Angew. Chem., Int. Ed.*, 2018, **57**, 16852; (f) J.-H. Jin, J. Zhao, W.-L. Yang and W.-P. Deng, *Adv. Synth. Catal.*, 2019, **361**, 1592.
- 17 For reviews on chiral *N,N*-dioxides, see: (a) X. H. Liu, L. L. Lin and X. M. Feng, *Acc. Chem. Res.*, 2011, **44**, 574; (b) X. H. Liu, L. L. Lin and X. M. Feng, *Org. Chem. Front.*, 2014, **1**, 298; (c) X. H. Liu, H. F. Zheng, Y. Xia, L. L. Lin and X. M. Feng, *Acc. Chem. Res.*, 2017, **50**, 2621; (d) X. H. Liu, S. X. Dong, L. L. Lin and X. M. Feng, *Chin. J. Chem.*, 2018, **36**, 791; (e) X. H. Liu and X. M. Feng, *Angew. Chem., Int. Ed.*, 2018, **57**, 16604; (f) Z. Wang, X. H. Liu and X. M. Feng, *Aldrichimica Acta*, 2020, **53**, 3; (g) M.-Y. Wang and W. Li, *Chin. J. Chem.*, 2021, **39**, 969.
- 18 For selected reviews on cyclobutanes as 1,4-dipoles, see: (a) F. de Nanteuil, F. De Simone, R. Frei, F. Benfatti, E. Serrano and J. Waser, *Chem. Commun.*, 2014, **50**, 10912; (b) H.-U. Ressig and R. Zimmer, *Angew. Chem., Int. Ed.*, 2015, **54**, 5009; (c) N. Vemula and B. L. Pagenkopf, *Org. Chem. Front.*, 2016, **3**, 1205. For selected examples, see: (d) A. Levens, A. Ametovski and D. W. Lupton, *Angew. Chem., Int. Ed.*, 2016, **55**, 16136; (e) L. K. B. Garve, A. Kreft, P. G. Jones and D. B. Werz, *J. Org. Chem.*, 2017, **82**, 9235; (f) L.-W. Feng, H. Xiong, P. Wang, L. Wang and Y. Tang, *Angew. Chem., Int. Ed.*, 2017, **56**, 3055; (g) J.-L. Hu, L. Zhou, L. Wang, Z. Xie and Y. Tang, *Chin. J. Chem.*, 2018, **36**, 47; (h) D. Tong, J. Wu, N. Bazinski, D. Koo, N. Vemula and B. L. Pagenkopf, *Chem.-Eur. J.*, 2019, **25**, 15244; (i) M. Yamazaki, T. Yoshimura and J. Matsuo, *Tetrahedron Lett.*, 2021, **64**, 151804.
- 19 When the racemic reaction (Table 1, entry 1) was carried out at 0 °C, the [2+2] cycloaddition product was detected. Therefore, we deemed that the formal [4+2] adduct was generated from the transformation of the [2+2] cycloaddition product. See ESI, Table S1† entry 15 for details.
- 20 CCDC 2042864 (**3aa**), CCDC 2052253 (**rac-4ka**) and CCDC 2079315 (**rac-5aa**).†
- 21 Performing the reaction with a one-pot procedure resulted in **4** as the major product, See ESI, Table S5† for more details.
- 22 K. Zheng, X. H. Liu, J. N. Zhao, Y. Yang, L. L. Lin and X. M. Feng, *Chem. Commun.*, 2010, **46**, 3771.
- 23 For reviews of deprotection of Boc-protected amides using Lewis acids, see: (a) K. Jarowicki and P. Kociński, *J. Chem. Soc., Perkin Trans. 1*, 1999, **1**, 1589; (b) G. Sartori, R. Ballini, F. Bigi, G. Bosica, R. Maggi and P. Righi, *Chem. Rev.*, 2004, **104**, 199. For selected examples, see: (c) J. A. Stafford, M. F. Brackeen, D. S. Karanewsky and N. L. Valvano, *Tetrahedron Lett.*, 1993, **34**, 7873; (d) Z.-Y. Wei and E. E. Knaus, *Tetrahedron Lett.*, 1994, **35**, 847; (e) H. Kotsuki, T. Ohishi, T. Araki and K. Arimura, *Tetrahedron Lett.*, 1998, **39**, 4869.

